EARTHQUAKE ENGINEERING AND STRUCTURAL DYNAMICS
Earthquake Engng Struct. Dyn. 2002; **31**:515–538 (DOI: 10.1002/eqe.142)

Inelastic deformation response of SDOF systems subjected to earthquakes

Rafael Riddell[1,*,†], Jaime E. Garcia[2] and Eugenio Garces[1]

[1]*Department of Structural and Geotechnical Engineering, Universidad Católica de Chile, Santiago, Chile*
[2]*Department of Civil Engineering, Universidad de Cuenca, Azuay, Ecuador*

SUMMARY

Performance-based seismic design requires reliable methods to predict earthquake demands on structures, and particularly inelastic deformations, to ensure that specific damage-based criteria are met. Several methods based on the response of equivalent linear single-degree-of-freedom (SDOF) systems have been proposed to estimate the response of multi-degree-of-freedom structures. These methods do not offer advantages over the traditional Veletsos–Newmark–Hall (VNH) procedure, indeed, they have been shown to be inaccurate. In this study, the VNH method is revised, considering the inelastic response of elastoplastic, bilinear, and stiffness-degrading systems with 5% damping subjected to two sets of earthquake ground motions. One is an ensemble of 51 earthquake records in the Circumpacific Belt, and the other is a group of 44 records in California. A statistical analysis of the response data provides factors for constructing VNH inelastic spectra. Such factors show that the 'equal-displacement' and 'equal-energy' rules to relate elastic and inelastic responses are unconservative for high ductilities in the acceleration- and velocity-sensitive regions of the spectrum. It is also shown that, on average, the effect of the type of force–deformation relationship of non-linear systems is not significant, and responses can be conservatively predicted using the simple elastoplastic model. Copyright © 2001 John Wiley & Sons, Ltd.

KEY WORDS: performance-based design; inelastic deformation; earthquake response; non-linear response; inelastic spectrum

INTRODUCTION

After the great deal of damage caused by earthquakes in the last 10 or 15 years, there seems to be agreement that changes in the seismic design process are necessary to permit the construction of structures with predictable seismic performance. A performance objective represents a specific risk, stated in terms of the desired structural behavior (damage state) associated with a specific level ofearthquake demand (seismic hazard). Performance-based seismic design

* Correspondence to: Rafael Riddell, Department of Structural and Geotechnical Engineering, Universidad Católica de Chile, Vicuna Mackenna 4860, Santiago, Chile.
† E-mail: riddell@ing.puc.cl

Contract/grant sponsor: FONDECYT; contract/grant No: 1990112.

Received 15 January 2001
Revised 31 August 2001
Accepted 31 August 2001

requires reliable methods to analyze, design, and verify structures to ensure that selected performance goals are met. For this purpose, advanced techniques will have to be incorporated in future design procedures. Verification of the seismic performance of a structure by means of non-linear 3-D response–history analysis is possible today, however, significant improvement and standardization of this procedure, and the software required, are necessary to allow general use by the profession. A great difficulty for non-linear analysis is the limited understanding of the inelastic properties of structures, so that there are no generally accepted mathematical models for structural members, specially for reinforced concrete members in their various forms (walls, columns, joints) and predominant types of behaviour (shear, flexure–compression interaction). Besides modelling the hysteretic load–deformation behaviour, limit or collapse states need to be identified and defined, including disruption of concrete members due to crushing, punching shear, bond or anchorage failure, and fracture of welds and local buckling of steel members. Furthermore, a realistic non-linear building model should include the foundations and surrounding soil. Extensive discussion of these topics can be found elsewhere [1–3].

Until more sophisticated analysis procedures become generally available, simpler approaches are necessary. A simplified non-linear analysis procedure is the push-over method, in which the structure is subjected to a monotonically increasing lateral load of prescribed pattern; the structure progressively degrades, as structural members sequentially plastify, until it reaches a limit state or collapse condition. The incremental static analysis permits to determine the global force–displacement relationship of the building, or *capacity curve* [4], in terms of the total lateral force (base shear) and the lateral deflection of the roof. The strengths of this method are its simplicity and its potential to expose weak links in the structure; its weakness is the questionable validity of a fixed lateral load pattern associated to only one mode of vibration of the structure.

The capacity curve is then converted to a *capacity diagram* or force–deformation relationship of a simplified SDOF representation of the multi-degree building. In order to determine compliance with a given performance level, the displacement response of the building due to a given earthquake demand must be determined. The ATC-40 document [4] proposes approximate methods to estimate the non-linear response of SDOF systems on the basis of the response of equivalently damped linear systems. Chopra and Goel [5] have pointed out several deficiencies of the ATC-40 procedures, including non-convergence, and have shown that deformations can be significantly underestimated over a wide range of system periods.

In the traditional VNH inelastic spectrum [6–13], the response of a non-linear SDOF system is directly read without iterations; in turn, the spectral ordinates are associated to known degrees of uncertainty, depending on the probability of exceedance of the factors selected to construct the spectrum. The earthquake demand (seismic hazard) is simply represented by the peak ground motion parameters: acceleration A, velocity V, and displacement D. Inelastic spectra can be constructed for a variety of situations and conditions, the only limitation being the quality and quantity of the ground motion data available to derive the factors for constructing the spectrum. The statistical procedure [12] used to obtain such factors is briefly summarized herein.

STRUCTURAL MODELS AND GROUND MOTIONS CONSIDERED

A simple SDOF system was used in this study, with force–deformation relationship given by three non-linear models: elastoplastic, bilinear, and stiffness degrading (Figure 1). These

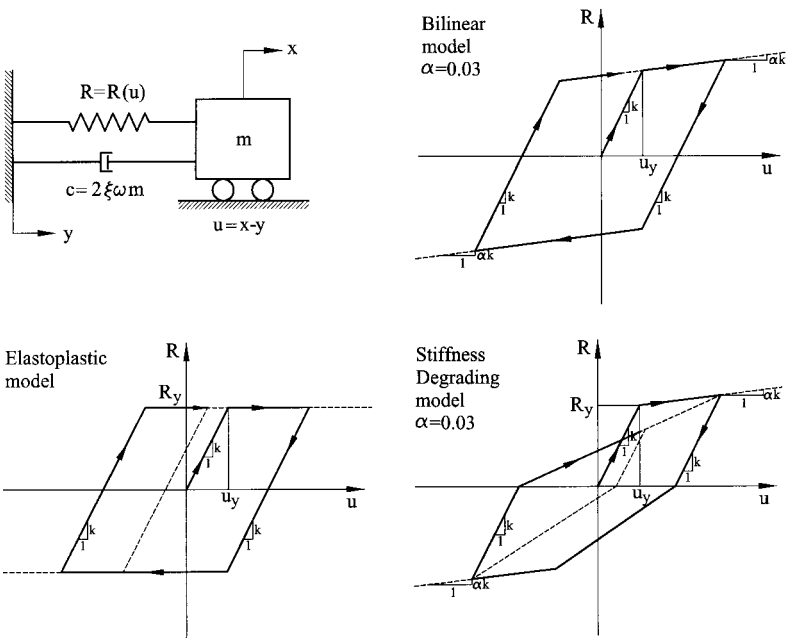

Figure 1. Single-degree-of-freedom system and non-linear load–deformation models used.

models cover a broad range of structural behaviour; they are intended to represent over all generic behavior, rather than specific characteristics of individual systems [12, 14]. Strength deterioration was not considered, mainly because in a well-detailed structure it should only occur at extreme deformations near the failure state. A damping factor $\xi = 0.05$, i.e. five per cent of critical, was used.

The Circumpacific Belt group of earthquake records used as input motions is presented in Table I. These records represent moderate to large intensities of motion. Most of the records listed in Table I meet at least two of the following conditions: structural damage was observed near the recording site, peak ground acceleration larger than $0.25g$, and peak ground velocity larger than 25 cm/s. It was not attempted to group the records according to similar characteristic regarding soil conditions, tectonic setting, Mercalli Intensity, distance to fault, or others; the reason was in part the lack of reliable data, on geotechnical information for example, and the difficulty to form groups of statistical significance. Naturally, owing to the heterogeneity of the group the results present larger scatter and the factors derived, a higher degree of uncertainty. Indeed, if families of records of similar characteristics were arranged, the underlying uncertainty should decrease and response estimates could be made more accurately. It must be pointed out however that the factors derived for this group of records are not intended to be directly extrapolated to very soft soils, since most of the ground motion data considered are on firm ground.

To form a group of records representative of California three types of earthquake events were analysed. The first type corresponds to large strike-slip earthquakes ($M_w > 7$) typically associated with major faults rupture, several meters of slip along the fault, and strong motion

Table I. Earthquake records in the Circumpacific Belt group.

Station, component, date	Maximum acceleration (g)	Maximum velocity (cm/s)	Maximum displacement (cm)
CMD Vernon, U.S.A., S08W (03/10/1933)	−0.133	−29.03	−19.50
El Centro, U.S.A., S00E (05/18/1940)	−0.348	−33.45	−12.36
Olympia, U.S.A., N86E (04/13/1949)	0.280	17.09	−9.38
Eureka, U.S.A., N79E (12/212/1954)	0.258	−29.38	−12.55
Ferndale, U.S.A., N44E (12/21/1954)	−0.159	−35.65	14.72
Kushiro Kisyo-Dai, Japan, N90E (04/23/1962)	0.478	−20.01	5.22
Ochiai Bridge, Japan, N00E (04/05/1966)	−0.276	23.66	8.36
Temblor, U.S.A., S25W (06/27/1966)	0.348	−22.52	−5.55
Cholame 2, U.S.A., N65E (06/27/1966)	0.489	78.08	−26.27
Cholame 5, U.S.A., N85E (06/27/1966)	0.434	25.44	−6.89
Lima, Peru, N08E (10/17/1966)	0.409	−15.20	−11.67
El Centro, U.S.A., S00W (04/08/1968)	0.130	−25.81	12.96
Hachinohe, Japan, N00E (05/16/1968)	0.269	−35.43	−9.68
Aomori, Japan, N00E (05/16/1968)	−0.257	−39.12	−19.97
Muroran, Japan, N00E (05/16/1968)	−0.220	30.28	7.90
Itajima Bridge, Japan, Long. (08/06/1968)	0.612	−22.56	−4.59
Itajima Bridge, Japan, Long. (09/21/1968)	−0.261	−12.93	−2.80
Toyohama Bridge, Japan, Long. (01/05/1971)	0.450	15.90	3.38
Pacoima, U.S.A., S16E (02/09/1971)	1.171	113.23	−41.92
Orion LA, U.S.A., N00W (02/09/1971)	0.255	30.00	16.53
Castaic, U.S.A., N21E (02/09/1971)	0.316	17.16	−5.05
San Juan, Argentina, S90E (11/23/1977)	0.193	−20.60	6.33
Ventanas, Chile, Trans. (11/07/1981)	0.268	−17.87	−8.04
Papudo, Chile, Long. (11/07/1981)	−0.603	−18.93	−7.43
La Ligua, Chile, Long. (11/07/1981)	−0.469	−18.83	4.49
Rapel, Chile, N00E (03/03/1985)	0.467	−21.64	−6.54
Zapallar, Chile, N90E (03/03/1985)	0.304	13.46	−1.69
Llo-Lleo, Chile, N10E (03/03/1985)	−0.712	−40.29	−10.49
Viña del Mar, Chile, S20W (03/03/1985)	0.363	30.74	−5.42
UTFSM, Chile, N70E (03/03/1985)	0.176	14.60	3.11
Papudo, Chile, S40E (03/03/1985)	0.231	12.41	1.60
Llay Llay, Chile, S10W (03/03/1985)	−0.352	−41.79	8.43
San Felipe, Chile, N80E (03/03/1985)	0.434	−17.77	−3.50
El Almendral, Chile, N50E (03/03/1985)	0.297	−28.58	−5.78
Melipilla, Chile, N00E (03/03/1985)	−0.686	34.25	12.02
Pichilemu, Chile, N00E (03/03/1985)	0.259	−11.68	3.73
Iloca, Chile, N90E (03/03/1985)	0.278	15.09	1.39
SCT, Mexico, N90E (09/19/1985)	−0.171	−60.61	21.16
Corralitos, U.S.A., N00E (10/18/1985)	0.630	−55.20	12.03
KSR Kushiro, Japan, N63E (01/15/1993)	0.725	33.59	4.73
Pacoima DAM, U.S.A., S05E (01/17/1994)	−0.415	44.68	4.65
Newhall, U.S.A., N00E (01/17/1994)	0.591	−94.73	28.81
Pacoima-Kagel, U.S.A., N00E (01/17/1994)	0.433	−50.88	−6.64
Sylmar, U.S.A., N00E (01/17/1994)	0.843	−128.88	−30.67
Santa Monica, U.S.A., N90E (01/17/1994)	−0.883	41.75	−15.09
Moorpark, U.S.A., S00E (01/17/1994)	0.292	20.28	4.67
Castaic, U.S.A., N90E (01/17/1994)	0.568	−51.51	−9.19

Table I. (*Continued*).

Station, component, date	Maximum acceleration (g)	Maximum velocity (cm/s)	Maximum displacement (cm)
Arleta, U.S.A., N90E (01/17/1994)	0.344	−40.37	8.36
Century City-LA, U.S.A., N90E (01/17/1994)	0.256	21.36	−6.51
Obregon Park-LA, U.S.A., N00E (01/17/1994)	−0.408	−30.86	−2.65
Hollywood-LA, U.S.A., N00E (01/17/1994)	−0.389	22.26	4.27

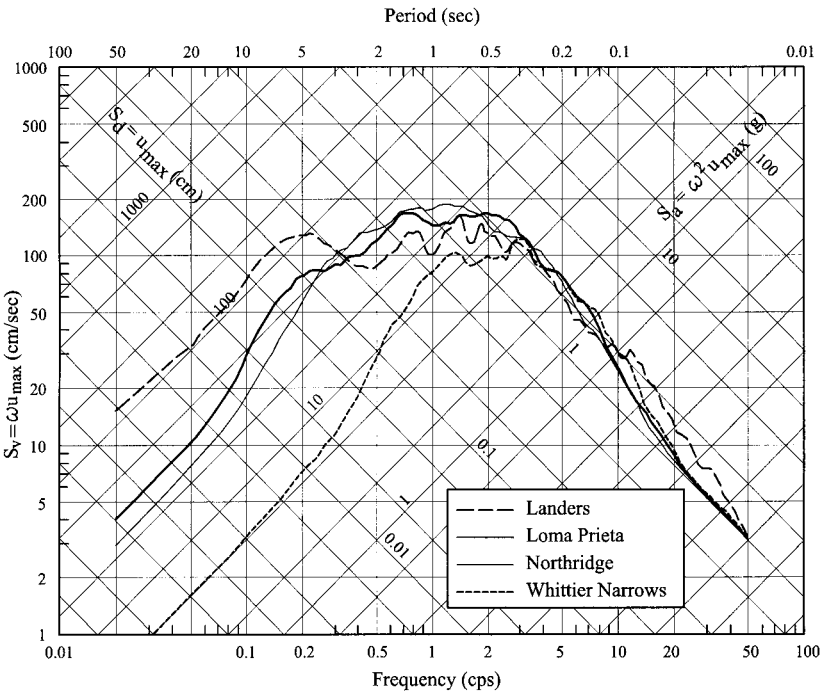

Figure 2. Average of spectra normalized to peak ground acceleration for four California earthquakes. Elastic systems with 5 per cent damping.

duration from 20 to 30 s. Representative of this type, although not the greatest that can be expected, is the 1992 Landers earthquake: $M_w = 7.2$ ($M_s = 7.5$), rupture length of about 70 km, and largest surface offset of about 6.4 m [15]. Figure 2 shows the average elastic response spectrum—normalized to peak ground acceleration—for four records of the Landers earthquake (stations at Coolwater and Lucern with both components of each). These records were baseline adjusted with a procedure specially devised to recover long period information [16]. The spectrum shape reveals an important content of long period waves, which are of course related to large ground displacements. Although there is an abundant set of strong motion recordings of the Landers earthquake, no data are available on similar or stronger events of this kind

to permit to form a statistically significant group. The second type of California earthquakes corresponds to moderate magnitude events, like the 1989 Loma Prieta ($M_w = 6.9$, $M_s = 7.1$, no evidence of surface rupture but significant ground cracking, strong motion lasting less than 10 s), and the 1994 Northridge ($M_w = 6.7$, $M_s = 6.8$, no surface faulting, about 10 s of strong motion duration). Average normalized spectra for Loma Prieta (24 records, see Table II) and Northridge (20 records) are shown in Figure 2. The spectra are quite similar, except perhaps for the more important long period content of the Loma Prieta spectrum. These earthquakes should not be considered rare events in California; indeed, the intensity of the Northridge motions corresponds to a probability of exceedance larger than the design (code) motions [17], i.e. they are adequate to check structural performance of code designed structures. For this reason, and due to the similarity of their average spectra, the Loma Prieta and Northridge records (44 total) were combined in the California group (Table II) considered in this study. The third type of earthquakes in California is represented by the 1987 Whittier Narrows event, $M_w = 6$. The average spectrum for 10 records obtained during this earthquake (stations at Alhambra, Altadena, LA-116th St., LA-Obregon Park, and Tarzana, with two components each) clearly presents narrower frequency content and lower amplification—except in the acceleration region—than the previously discussed types of earthquakes (Figure 2). Thus, these weaker records were discarded for this study.

RESPONSE CALCULATIONS AND STATISTICAL ANALYSIS OF THE DATA

The equation of motion of the system shown in Figure 1 can be written as

$$\ddot{u}(t) + 2\xi\omega\dot{u}(t) + \frac{R(u)}{m} = -\ddot{y}(t) \tag{1}$$

where u is the relative displacement of the mass m with respect to its base, $\omega = \sqrt{k/m}$ is the undamped elastic circular frequency, $R(u)$ is the hysteretic restoring force with stiffness parameter k (Figure 1), $\xi = c/2\omega m$ is the damping factor as a fraction of the critical value, and $\ddot{y}(t)$ is the base acceleration. Of course the use of the elastic frequency and elastic stiffness is only a conventional manner of identifying the various systems; certainly, the eventual period change or softening due to inelastic behaviour is accounted for in the response calculations. The resistance function is defined by the yield strength R_y and the yield deformation u_y, such that $R_y = ku_y = m\omega^2 u_y$. The response ductility μ is defined as the ratio of the maximum displacement, u_{max}, without taking into account the sign, over the yield displacement, i.e. $\mu = u_{max}/u_y$. One important property of Equation (1) is that $R(u)$ and $\ddot{y}(t)$ can be scaled by a constant and the response ductility does not change. In fact, if μ is the response ductility of a system with resistance function defined by R_y and u_y when subjected to the ground motion $\ddot{y}(t)$, the response of a new system with $R'_y = \lambda R_y$ and $u'_y = \lambda u_y$ subjected to a ground motion $\ddot{y}'(t) = \lambda\ddot{y}(t)$, with $\lambda =$ constant, is such that $\mu' = \mu$. The importance of this property is that it permits to scale or normalize the ground motions and the inelastic response spectra for the purpose of calculating the average amplifications for a family of records.

Responses were calculated for 250 different frequencies for each record, following an iterative procedure to obtain inelastic responses associated with the desired target ductility values of 1 (elastic), 1.5, 2, 3, 5 and 10. The results were presented in the form of tripartite logarithmic plots, as the spectra shown in Figure 3. In this case the abscissa is the frequency

Table II. Earthquake records in the California group.

Station, date	Comp	Maximum acceleration (g)	Maximum velocity (cm/s)	Maximum displacement (cm)
Arleta, Nordhoff Ave. Fire Station (01/17/1994)	N00E	0.308	−23.29	8.48
	N90E	0.344	−40.37	8.36
Castaic, Old Ridge Route (01/17/1994)	N00E	0.514	−52.56	−15.32
	N90E	0.568	−51.51	−9.19
Century City, L.A. (01/17/1994)	N00E	0.222	−25.07	6.25
	N90E	0.256	21.36	−6.51
Los Angeles, Hollywood Storage Gr. (01/17/1994)	N00E	−0.389	22.26	4.27
	N90E	0.232	−18.15	4.70
Los Angeles, Obregon Park (01/17/1994)	N00E	−0.408	−30.86	−2.64
	N90E	0.355	14.47	−4.16
Moorpark (01/17/1994)	N00E	0.292	20.28	4.67
	N90E	0.193	−20.37	4.11
Newhall, L.A. County Fire Station (01/17/1994)	N00E	0.591	−94.73	28.81
	N90E	−0.583	−74.84	16.75
Pacoima, Kagel Canyon (01/17/1994)	N00E	0.433	−50.88	−6.64
	N90E	0.301	−30.94	−10.96
Santa Monica, City Hall Gr. (01/17/1994)	N00E	−0.370	24.91	7.05
	N90E	−0.883	41.75	−15.09
Sylmar, County Hosp. Parking Lot (01/17/1994)	N00E	0.843	−128.89	−35.96
	N90E	0.604	−76.94	−15.99
Capitola, Fire Station (10/18/1989)	N00E	−0.472	36.15	12.07
	N90E	−0.399	30.71	−9.46
Corralitos, Eureka Canyon Rd. (10/18/1989)	N00E	0.630	−55.20	−11.85
	N90E	0.479	−47.50	−16.36
Gilroy #1, Gavilan College (10/18/1989)	N00E	0.435	31.92	7.34
	N90E	0.443	−33.84	7.88
Gilroy #2, Hwy 101/Bolsa Rd. Motel (10/18/1989)	N00E	−0.351	33.34	8.15
	N90E	0.323	−39.23	12.03
Gilroy #3, Gilroy Sewage Plant (10/18/1989)	N00E	−0.542	34.48	−7.31
	N90E	0.369	43.77	16.31
Gilroy #4, San Isidro School (10/18/1989)	N00E	−0.416	39.08	−7.72
	N90E	−0.214	38.18	9.42
Gilroy #7, Mantelli Ranch (10/18/1989)	N00E	0.210	16.58	2.71
	N90E	0.320	−16.31	3.58
Gilroy, Gavilan College. (10/18/1989)	N67E	0.356	28.92	6.86
	N23W	−0.316	22.96	5.81
Hollister, South St. and Pine Dr. (10/18/1989)	N00E	0.369	62.78	33.37
	N90E	−0.178	−30.89	−19.28
Santa Cruz, UCSC. (10/18/1989)	N00E	−0.442	21.23	−5.91
	N90E	0.409	21.23	−8.64
Saratoga, Aloha Ave. (10/18/1989)	N00E	−0.504	−41.35	16.21
	N90E	0.322	−43.61	27.95
San Francisco Int. Airport (10/18/1989)	N00E	−0.235	26.46	4.87
	N90E	−0.332	29.26	−5.81

($f = \omega/2\pi$), but the period ($T = 1/f$) may be simultaneously read as well since a plot with T as abscissa is a mirror image of the former. This type of plot, named inelastic yield spectrum (IYS) [12], or constant ductility spectrum [18], features in the displacement axis the yield

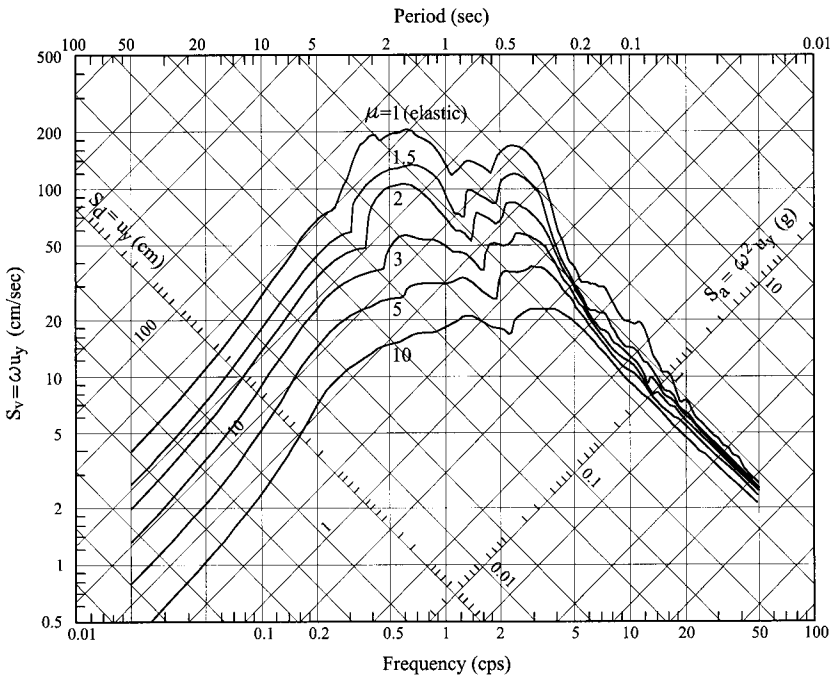

Figure 3. Inelastic yield spectra for stiffness degrading systems with 5 per cent damping subjected to the Sylmar record, N00E, 01/17/94.

deformation u_y necessary to limit the maximum deformation u_{max} of the system so that the target ductility μ is not exceeded. The acceleration axis, at 90° clockwise from the displacement axis, features the quantity $\omega^2 u_y$, which multiplied by the mass of the system gives the yield strength R_y. In the tripartite logarithmic plot the spectral quantities in the displacement, velocity, and acceleration axes are interrelated; indeed, denoting them by S_d, S_v and S_a, respectively, the relationship $S_a = \omega S_v = \omega^2 S_d$ holds. By virtue of the aforementioned property of Equation (1), and the manner in which the IYS is constructed, the IYS can be directly scaled or normalized by a constant factor λ, which is equivalent to a parallel shift of the spectral ordinates in the vertical direction.

The purpose of the statistical analysis is to determine factors for constructing design spectra when estimates can be made of the possible peak ground motion parameters for future earthquakes affecting a site. The parameters A, V and D control the response over three regions of the spectrum and provide a better basis for characterizing design spectra than using only one. Figure 4(a) shows the elastic pseudo-acceleration response S_a of a rigid system ($f = 5$ cps) versus peak ground acceleration A for the 51 Circumpacific records. It is apparent that such variables are linearly correlated, therefore rational estimates of the response to a specified earthquake demand can be made if statistics of the random variable S_a/A (acceleration response amplification) are known. Similarly, Figure 4(c) shows that the displacement response S_d of a rather flexible system ($f = 0.33$ cps) and peak ground displacement D are correlated, thus, response estimates can be made if the random variable S_d/D is studied. The same can

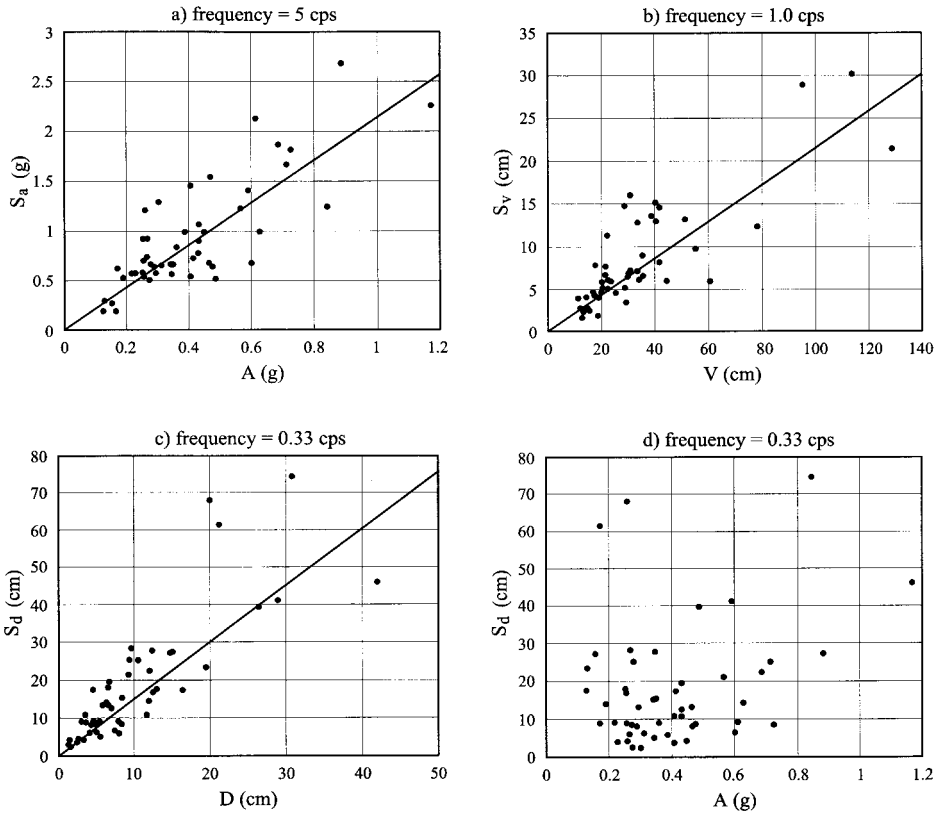

Figure 4. Correlation between responses and peak ground motion parameters. Data for the Circumpacific Belt group of records.

be said for the variable S_v/V in the intermediate frequency region (Figure 4(b)). The previous observations are well known and perhaps widely accepted. But, what may not be so clearly understood is that displacement responses (S_d) of flexible systems are not correlated with peak ground acceleration (A) as shown in Figure 4(d), therefore, S_d for such systems cannot be estimated from average spectra normalized to peak ground acceleration.

In summary, the statistical analysis consists in determining factors ψ_μ which, applied to the ground motion estimates p_g, give the spectral ordinates S_μ for each of the three characteristic regions of the spectrum:

$$S_\mu = \psi_\mu p_g \tag{2}$$

where p_g represents A, V or D depending on the spectral region under consideration. Alternatively, the inelastic spectrum S_μ can be obtained by de-amplifying the elastic spectrum S_e, so that

$$S_\mu = \phi_\mu S_e \tag{3}$$

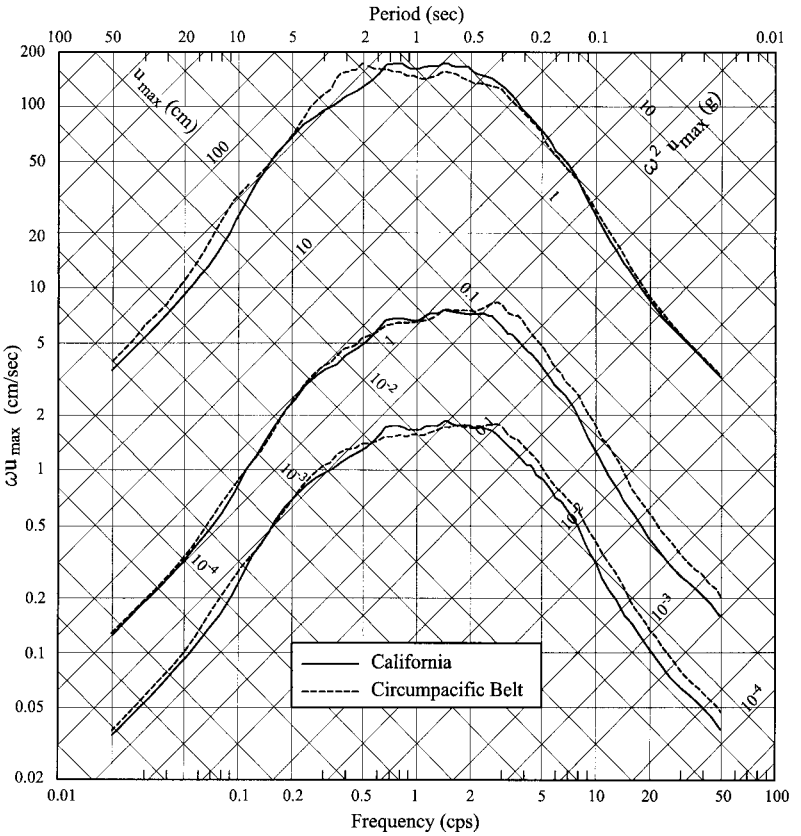

Figure 5. Average of spectra normalized to peak ground acceleration, displacement and velocity. Elastic systems with 5 per cent damping.

where the de-amplification factor ϕ_μ obviously corresponds to the ratio $\psi_\mu/\psi_{\mu=1}$ and S_e corresponds to the particular case of $S_{\mu=1}$. It is worth commenting here that Equation (3) is often misunderstood as equivalent to 'derive inelastic spectra from elastic response analyses'; this is certainly not the case because actual inelastic responses directly lead to the ψ_μ factors from which the ϕ_μ factors are obtained.

The methodology, presented in detail by Riddell and Newmark [12], is briefly described herein:

(a) As a first step in the analysis the spectra for each record is independently normalized with respect to its three peak ground motion parameters, so that the ith record is normalized to peak ground acceleration $A_i = 1$, to peak ground velocity $V_i = 1$, and to peak ground displacement $D_i = 1$. Then, responses are computed for a number of records and statistics of the normalized responses are evaluated at each frequency. Figure 5 shows the average spectra normalized to peak ground acceleration, displacement and velocity, from top to bottom, respectively, for the two groups of records considered in

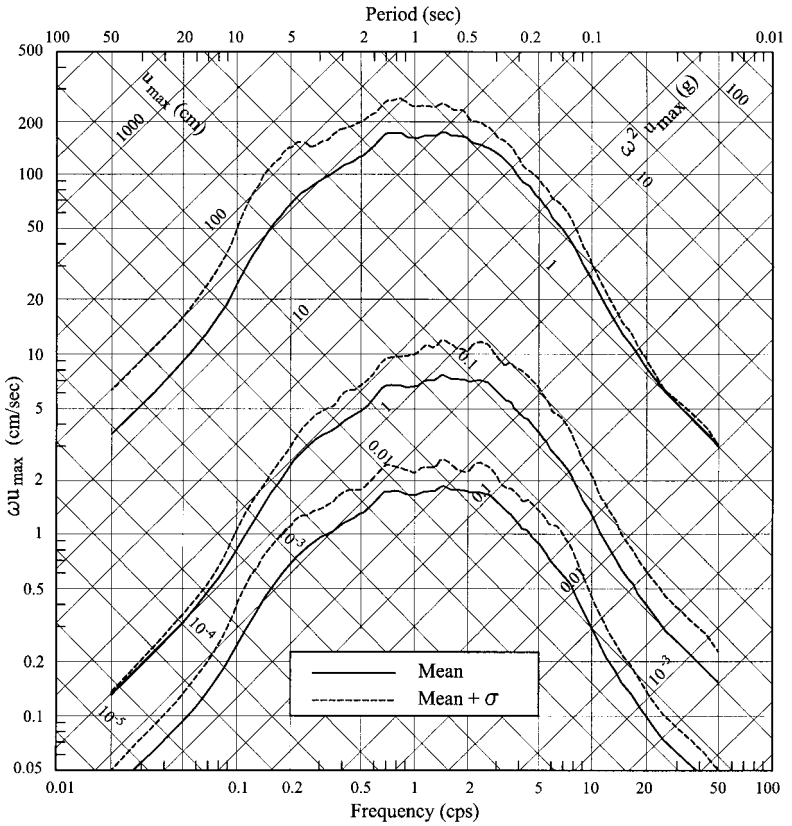

Figure 6. Mean and mean plus one standard deviation of normalized spectra for the California group of records. Elastic systems with 5 per cent damping.

this study. The average spectra feature segments that present approximately constant response amplification with respect to the corresponding peak ground motion parameters, thus making it possible to identify a region of spectral acceleration amplification, a region of spectral velocity amplification, and a region of displacement amplification. Henceforth these spectral regions will be simply referred to as acceleration, velocity and displacement regions. Incidentally, in Figure 5, the similarity of the average spectra for both groups of records is apparent (note that this comparison is to be made in the spectral region associated with the normalization parameter of the spectra). In turn, as illustrated by Figure 6, the standard deviation at each frequency increases from high to low frequencies when the spectra are normalized to peak ground acceleration, whereas the opposite occurs for normalization to ground displacement. Normalization to ground velocity results in a more uniform standard deviation over the entire frequency range. The previous observations justify the procedure based in normalizing to three parameters independently in order to minimize the uncertainty in each spectral region.

(b) To eliminate arbitrariness in the determination of the spectral regions, a procedure [12] consisting in fitting trapezoidal lines to the mean spectra between fixed lower and upper frequency limits is used; these limits correspond to the beginning of the displacement region and the end of the acceleration region. In this study the lower frequency limit was chosen as 0.15 cps, and the upper frequency was fixed at 10 cps. The selection of these limits requires observation of the average elastic and inelastic spectra. However, it is worth pointing out that minor changes in these limits have a negligible effect on the final amplification factors.

(c) Finally, frequency-band statistics are computed within the determined spectral regions for the ensemble of normalized spectra, in such a way that statistics for the acceleration region are computed for the data normalized to peak ground acceleration, statistics in the velocity region are computed for data normalized to peak ground velocity, and correspondingly for the displacement region. The mean values correspond to the aforementioned ψ_μ factors, the standard deviation is designated by σ_μ, and the coefficient of variation by $\Omega_\mu = \sigma_\mu/\psi_\mu$.

DISCUSSION OF RESULTS OF THE STATISTICAL ANALYSIS

The calculated frequency-band statistics are summarized in Tables III–V for the Circumpacific Belt group and in Table VI for the California group. It can be seen that the factors for elastoplastic systems are very similar to those of bilinear and stiffness-degrading systems. In this regard, it is instructive to compare the average spectra for the three types of load-deformation

Table III. Factors for constructing elastic and inelastic demand spectra for elastoplastic systems with 5 per cent damping. Circumpacific Belt records.

Spectral region	Ductility μ	ψ_μ	σ_μ	COV	ϕ_μ
	1.0	1.742	0.776	0.446	1.000
	1.5	1.058	0.452	0.427	0.608
Displacement	2.0	0.756	0.326	0.431	0.434
	3.0	0.499	0.228	0.457	0.286
	5.0	0.301	0.142	0.472	0.173
	10.0	0.148	0.072	0.488	0.085
	1.0	1.695	0.773	0.456	1.000
	1.5	1.058	0.417	0.394	0.624
Velocity	2.0	0.794	0.310	0.390	0.468
	3.0	0.547	0.211	0.386	0.322
	5.0	0.365	0.134	0.367	0.216
	10.0	0.224	0.080	0.356	0.132
	1.0	2.100	0.701	0.334	1.000
	1.5	1.469	0.379	0.258	0.699
Acceleration	2.0	1.238	0.287	0.232	0.589
	3.0	1.020	0.221	0.217	0.486
	5.0	0.841	0.181	0.215	0.400
	10.0	0.671	0.159	0.236	0.319

Table IV. Factors for constructing elastic and inelastic demand spectra for bilinear systems with 5 per cent damping. Circumpacific Belt records.

Spectral region	Ductility μ	ψ_μ	σ_μ	COV	ϕ_μ
Displacement	1.0	1.742	0.776	0.446	1.000
	1.5	1.056	0.446	0.423	0.606
	2.0	0.745	0.312	0.420	0.427
	3.0	0.474	0.205	0.432	0.272
	5.0	0.271	0.111	0.411	0.156
	10.0	0.120	0.044	0.367	0.069
Velocity	1.0	1.695	0.773	0.456	1.000
	1.5	1.043	0.397	0.381	0.615
	2.0	0.764	0.282	0.369	0.451
	3.0	0.503	0.174	0.347	0.296
	5.0	0.317	0.102	0.322	0.187
	10.0	0.182	0.053	0.293	0.107
Acceleration	1.0	2.100	0.701	0.334	1.000
	1.5	1.442	0.366	0.253	0.687
	2.0	1.195	0.262	0.220	0.570
	3.0	0.958	0.198	0.206	0.456
	5.0	0.759	0.154	0.203	0.361
	10.0	0.568	0.125	0.220	0.271

Table V. Factors for constructing elastic and inelastic demand spectra for stiffness degrading systems with 5 per cent damping. Circumpacific Belt records.

Spectral region	Ductility μ	ψ_μ	σ_μ	COV	ϕ_μ
Displacement	1.0	1.742	0.776	0.446	1.000
	1.5	1.031	0.420	0.408	0.592
	2.0	0.707	0.271	0.384	0.406
	3.0	0.431	0.157	0.364	0.248
	5.0	0.243	0.085	0.349	0.139
	10.0	0.113	0.037	0.332	0.065
Velocity	1.0	1.695	0.773	0.456	1.000
	1.5	1.006	0.395	0.393	0.594
	2.0	0.727	0.266	0.366	0.429
	3.0	0.492	0.171	0.347	0.290
	5.0	0.327	0.103	0.316	0.193
	10.0	0.196	0.056	0.286	0.115
Acceleration	1.0	2.100	0.701	0.334	1.000
	1.5	1.424	0.347	0.244	0.678
	2.0	1.188	0.239	0.201	0.566
	3.0	0.994	0.172	0.173	0.473
	5.0	0.830	0.139	0.168	0.395
	10.0	0.654	0.127	0.194	0.311

Table VI. Factors for constructing elastic and inelastic demand spectra for elastoplastic systems with 5 per cent damping. Californian records.

Spectral region	Ductility μ	ψ_μ	σ_μ	COV	ϕ_μ
	1.0	1.705	0.647	0.380	1.000
	1.5	1.051	0.387	0.368	0.617
Displacement	2.0	0.753	0.268	0.356	0.441
	3.0	0.490	0.188	0.383	0.288
	5.0	0.293	0.120	0.407	0.172
	10.0	0.142	0.060	0.421	0.084
	1.0	1.738	0.650	0.374	1.000
	1.5	1.078	0.341	0.317	0.620
Velocity	2.0	0.803	0.247	0.307	0.462
	3.0	0.551	0.170	0.308	0.317
	5.0	0.368	0.113	0.306	0.212
	10.0	0.222	0.066	0.295	0.128
	1.0	2.159	0.682	0.316	1.000
	1.5	1.490	0.394	0.265	0.690
Acceleration	2.0	1.227	0.279	0.227	0.568
	3.0	0.997	0.191	0.191	0.462
	5.0	0.813	0.139	0.171	0.377
	10.0	0.643	0.119	0.185	0.298

relationships, as shown in Figures 7 and 8. Differences occur mainly for intermediate frequencies and large ductilities, and, most importantly, use of the elastoplastic idealization provides essentially always a conservative estimate of the average response.

The COV values in Table VI are similar to those found in previous studies. Riddell and Newmark [12] found COVs in the range 0.18–0.22 in the acceleration region of the spectrum, 0.31–0.39 in the velocity region, and 0.41–0.49 in the displacement region, for μ between 1 and 10. For Chilean earthquake data, Riddell [19] obtained COVs between 0.19–0.31, 0.25–0.4, and 0.33–0.44 in the mentioned regions, respectively, for the same damping and range of μ. Newmark and Hall [13] and Mohraz *et al.* [20] presented amplification factors for elastic systems with 5 per cent damping associated with basically the same COVs of about 0.26, 0.4 and 0.45 in the acceleration, velocity, and displacement regions respectively. The COV values in Tables III–V are in general larger than those in Table VI, as can be expected due to the heterogeneity of the Circumpacific Belt family.

Simple approximations for the ϕ_μ factors have been widely used after first introduced by Veletsos and Newmark [6, 7]. They are based on the well-known 'equal-displacement' and 'equal-energy' rules to relate elastic and inelastic responses, which lead to the ratios $1/\mu$ for the displacement and velocity regions, and $1/\sqrt{2\mu-1}$ for the acceleration region. In Figure 9 the actual ϕ_μ factors for elastoplastic systems for both groups of records are compared with the previously mentioned 'old rules' in the three spectral regions of interest. It is concluded that the old rules are unconservative (underestimate inelastic displacements) in the velocity region for systems with response ductility larger than 3, and in the acceleration region for $\mu > 2$. The following new rules, that present better fit to the computed ϕ_μ factors are recommended: $\phi_\mu = \mu^{-1.08}$ in the displacement region, $\phi_\mu = (1.9\mu - 0.9)^{-0.7}$ in the velocity

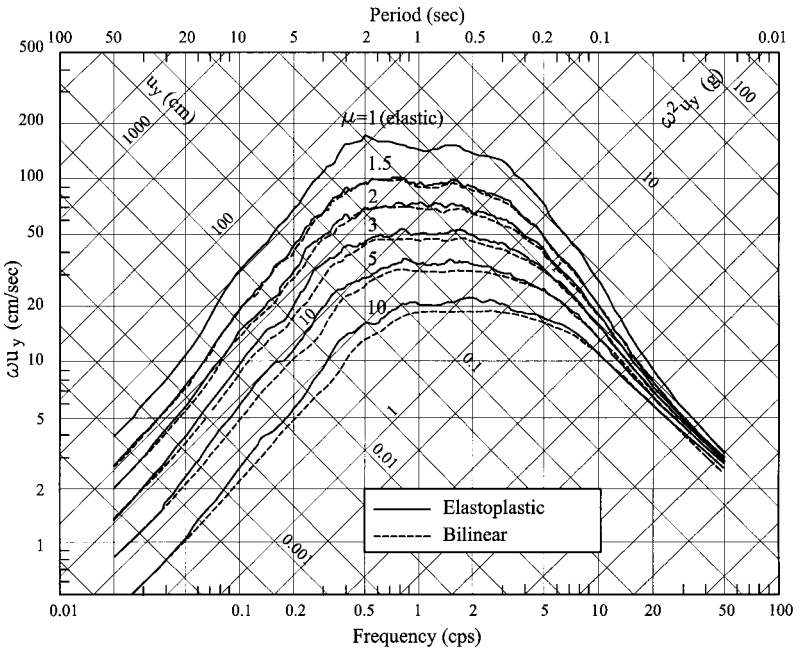

Figure 7. Average of IYS normalized to peak ground acceleration for the Circumpacific Belt group of records. Elastoplastic and bilinear systems with 5 per cent damping.

region and $\phi_\mu = (4.2\mu - 3.2)^{-1/3}$ in the acceleration region. Nevertheless, in the displacement region, the $1/\mu$ ratio can still be used since it is conservative, approximate enough, and attractive for its simplicity. It is worth pointing out that the previous exponential relationships have been derived for ϕ_μ factors that correspond to average conditions; factors associated to smaller probabilities of exceedance are not exactly the same, however, it was found that the differences are not large and the former can be used conservatively. Also worth noting is the similarity of the ϕ_μ factors for the Circumpacific Belt and California groups (Figure 9), suggesting that these factors have certain degree of generality that possibly makes them applicable regardless of the tectonic environment.

CONSTRUCTION OF DEMAND SPECTRA AND ESTIMATION OF INELASTIC DEFORMATIONS

The earthquake demand, or intensity of the ground shaking for the site under consideration, needs to be specified in terms of A, V, and D, the peak ground motion parameters. These parameters may have been determined by a specific seismic hazard analysis, or may be consistent with a code design spectrum, or may have been specified for a particular facility with special design requirements. The parameters must take into account specific conditions such as near-field effects, nearness to active faults, and site geology. The parameters may also be associated with various levels of the earthquake hazard: serviceability earthquake, design

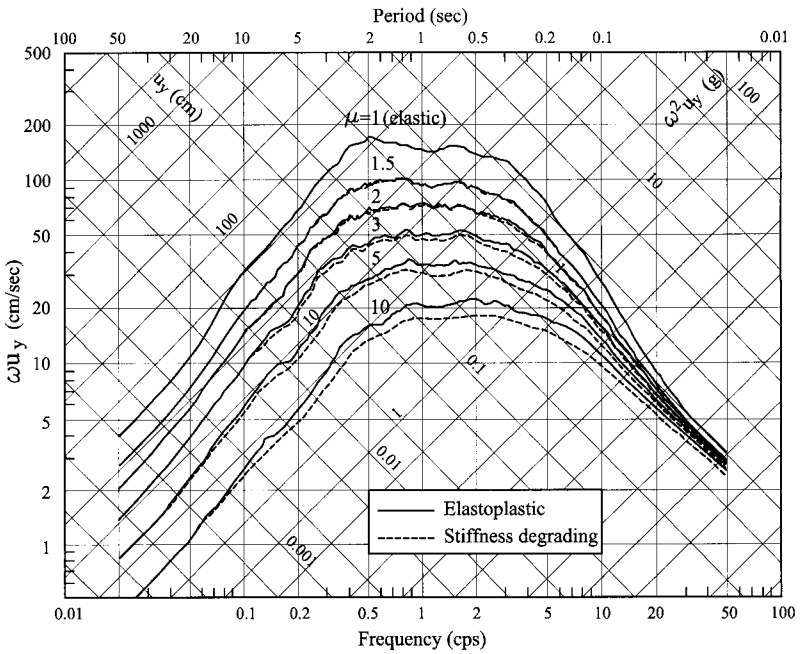

Figure 8. Average of IYS normalized to peak ground acceleration for the Circumpacific Belt group of records. Elastoplastic and stiffness degrading systems with 5 per cent damping.

earthquake, and maximum earthquake [4]. Discussion of the criteria for specification of the seismic hazard is beyond the scope of this paper.

The construction of demand spectra is illustrated in Figure 10, using the factors given in Tables III–VI. A, V, and D are drawn in a tripartite logarithmic plot, and the segments JK, KL and LM of the elastic spectrum are determined by amplifying the ground motion parameters by the $\psi_{\mu=1}$ factors corresponding to the three spectral regions. The limiting frequencies f_{I}, f_{J}, f_{M}, and f_{N} need to be set for each case. In this study, the following values were found appropriate for the data considered: $f_{\mathrm{I}} = 0.05$, $f_{\mathrm{J}} = 0.15$, $f_{\mathrm{M}} = 10$, and $f_{\mathrm{N}} = 30$. The elastic design spectrum is completed with the transition lines IJ and MN. To construct inelastic spectra, factors ψ_μ for the desired ductility factor μ are applied to the ground motion maxima to determine segments J′K′, K′L′, and L′M′ (conversely, the elastic design spectrum may be deamplified by the given factors ϕ_μ). Point I′ is determined by dividing the elastic ordinate at I by μ. Point N′ may be conservatively taken coincident with point N; however, based on actual response spectra, the factor $\mu^{-\eta}$ may be used to pass from N to N′, with $\eta = 0.11$, 0.13, and 0.15 for elastoplastic, stiffness degrading, and bilinear systems, respectively. When the ordinate of point L′ results lower than the design ground acceleration A, L′ may be joined directly to N′.

If a greater degree of conservatism is desired, factors associated with smaller probabilities of exceedance can be used. In other words, one is interested in p-percentile $\psi_{p\mu}$ factors, so that the probability that the response amplification will not exceed $\psi_{p\mu}$ is p. Assuming normal distribution, the percentile amplification factors are computed as $\psi_{p\mu} = \psi_\mu + \delta_p \sigma_\mu$, where the coefficient δ_p, which indicates the deviation from the mean, can be obtained from tables of

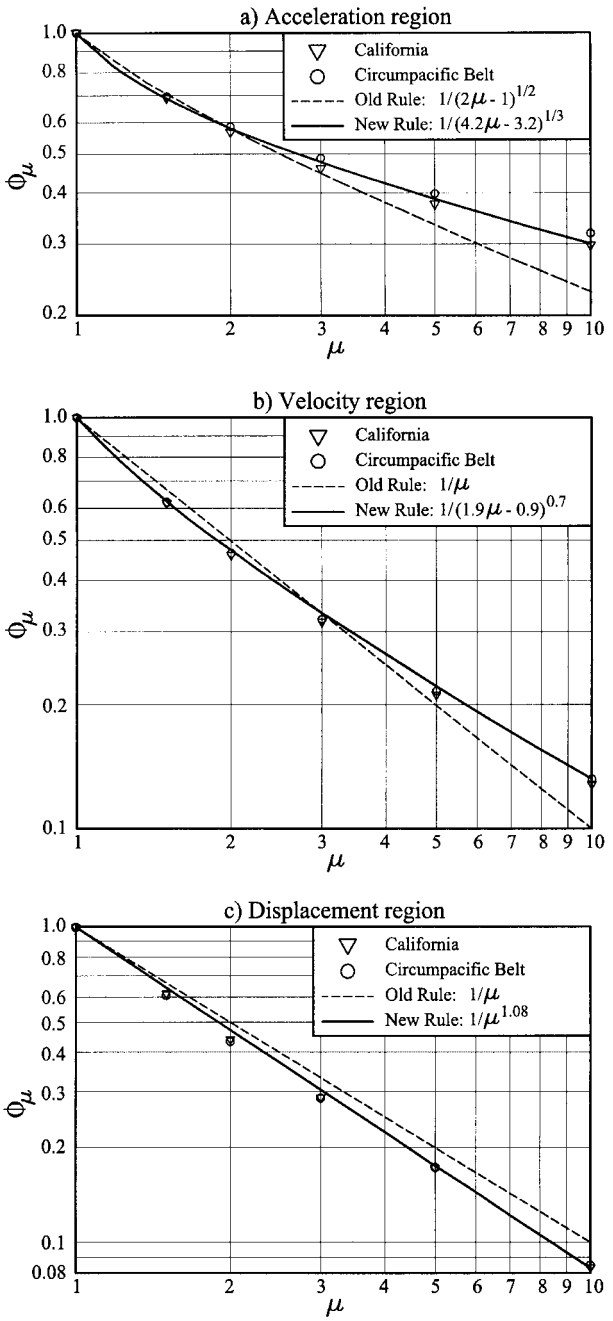

Figure 9. Deamplification factor versus ductility relationships in the three spectral regions. Elastoplastic systems with 5 per cent damping.

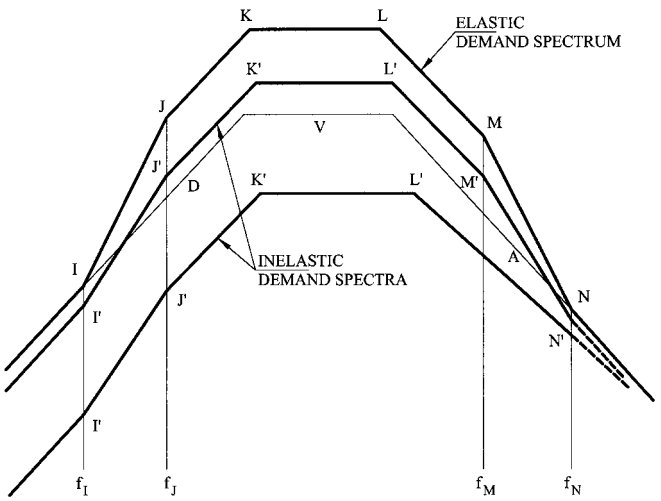

Figure 10. Construction of demand spectra.

standard normal probability. For instance, δ_p is equal to 0, 1, and 2 for p equal to 0.5, 0.841, and 0.977, respectively, and the associated $\psi_{p\mu}$ factors correspond to the 50-percentile, 84.1-percentile and 97.7-percentile values. Use of 84.1-percentile factors, i.e. 0.159 probability of exceedance are recommended.

CALIFORNIA GROUP: NEAR-FIELD AND SOIL EFFECTS

A study of near-field effects and the influence of geotechnical conditions on the factors to derive demand spectra was carried out. A summary of the observations made in the study is presented here, since space limitations do not permit detailed elaboration.

To analyse near-field effects, the California group was divided in two sets: one set containing records on sites within 15 km from the fault or rupture plane, and the other containing records on sites farther than 15 km. Owing to the number of records in the aggregated group, a finer segregation was not feasible.

In terms of average peak ground motion parameters, the intensity of motion of the nearer subgroup was larger than that of the other subgroup. The average V/A ratio was 96 cm/s/g for the California group, 102 for the near group and 90 for the distant group. The behaviour of the average V/A ratio with distance was not consistent. A value of 123 cm/s/g was obtained for the near-field records of the Northridge earthquake, and a value of 78 for the far group of Northrigde records; the opposite occurred for the Loma Prieta records, with averages of 90 and 107 for the near and far groups, respectively. The average AD/V^2 ratio was 3.2 for the aggregated California group, with values of 3 and 3.4 for the near and far subgroups respectively. The average AD/V^2 ratio for Northrigde records was 3, with values of 2.2 and 3.5 for the near-field and distant groups, respectively. Average AD/V^2 ratios for the Loma Prieta records separated in near and far subgroups presented almost no difference; the average ratio for the complete group was 3.4.

Average elastic spectra normalized to peak ground acceleration and velocity for the near and distant subgroups of the Californian group showed insignificant differences. Average spectra normalized to peak ground displacement did not present significant differences, but the average spectrum for the distant subgroup was larger than average spectrum for the near subgroup for all periods.

The ψ_μ factors given in Table VI can be conservatively used to construct demand spectra for near-field conditions, with errors that do not exceed 2.5 per cent in the displacement region, 3.5 per cent in the velocity region, and 1.7 per cent in the acceleration region. On the contrary, if the mentioned ψ_μ factors are used to construct demand spectra for sites farther than 15 km, errors of the same order will be made but on the unconservative side.

According to the soil conditions at the sites, the California group was divided into three subgroups, corresponding to the A, B and C USGS soil types. There are no records on very soft soils, thus the findings of this study cannot be extended to such type of soil. Factors for constructing demand spectra were obtained for the three subgroups and compared with the factors for the aggregated group given in Table VI. It was found that the latter are in general conservative, except for: soil type A in the acceleration region with differences less than 5 per cent, soil type B in the displacement region with differences up to 8 per cent, and soil type C in the velocity region with differences less than 6.4 per cent in the worst case. According to the previous information, it is concluded that the factors in Table VI can be used in general, making the indicated corrections if deemed necessary.

EXAMPLES

The examples presented in Section 8.3 of the ATC-40 report [4] are solved next using the method and data presented herein. The example building is a seven-storey reinforced concrete frame located in seismic zone 4 in California. Its fundamental period of vibration is 0.88 s. The capacity curve obtained from a push-over analysis of the building is shown in Figure 11(a). The corresponding capacity diagram—representing the first mode response of the building—is the curve ABCD shown in Figure 11(b) (the term 'capacity diagram' is used here instead of 'capacity spectrum' employed in ATC-40 since the latter is considered inappropriate). Figures 11(a) and 11(b) are adapted from the ATC-40 report. The conversion from one curve to the other is done by means of the following formula [4, 18]: $R/m = V/(\alpha_1 W)$, $\alpha_1 = L_1^2/M_1$, $L_1 = \phi_1^{\mathrm{T}}\mathbf{m}r$, $M_1 = \phi_1^{\mathrm{T}}\mathbf{m}\phi_1$, $F_1 = L_1/M_1$, $u = \Delta_{\mathrm{r}}/(F_1\phi_{1,\mathrm{roof}})$, where R is the resistance function of the equivalent SDOF system, V is the base shear of the building, W is the total weight of the building, α_1 is the effective modal mass associated with the fundamental mode shape ϕ_1 (which can be interpreted as the part of the total mass responding to the earthquake in the first mode), M_1 is the generalized mass corresponding to ϕ_1, $\mathbf{m}$ is the mass matrix, r is the displacement transformation vector, F_1 is the modal amplitude or participation factor associated with ϕ_1, $\phi_{1,\mathrm{roof}}$ is the component of ϕ_1 corresponding to the top storey, Δ_{r} is the roof displacement, and u is the displacement of the equivalent SDOF system.

The demand earthquake considered in the ATC-40 example is represented by the elastic design spectrum shown in Figure 11(c). Two sets of seismic coefficients [21] were used to illustrate the effect of different soil profiles: $C_{\mathrm{A}} = 0.4$ and $C_{\mathrm{V}} = 0.4$, and $C_{\mathrm{A}} = 0.44$ and $C_{\mathrm{V}} = 0.64$, the latter is the softer. These two cases will be dealt with in Examples 1 and 2, respectively. C_{A} represents the effective peak acceleration or design ground acceleration, i.e.

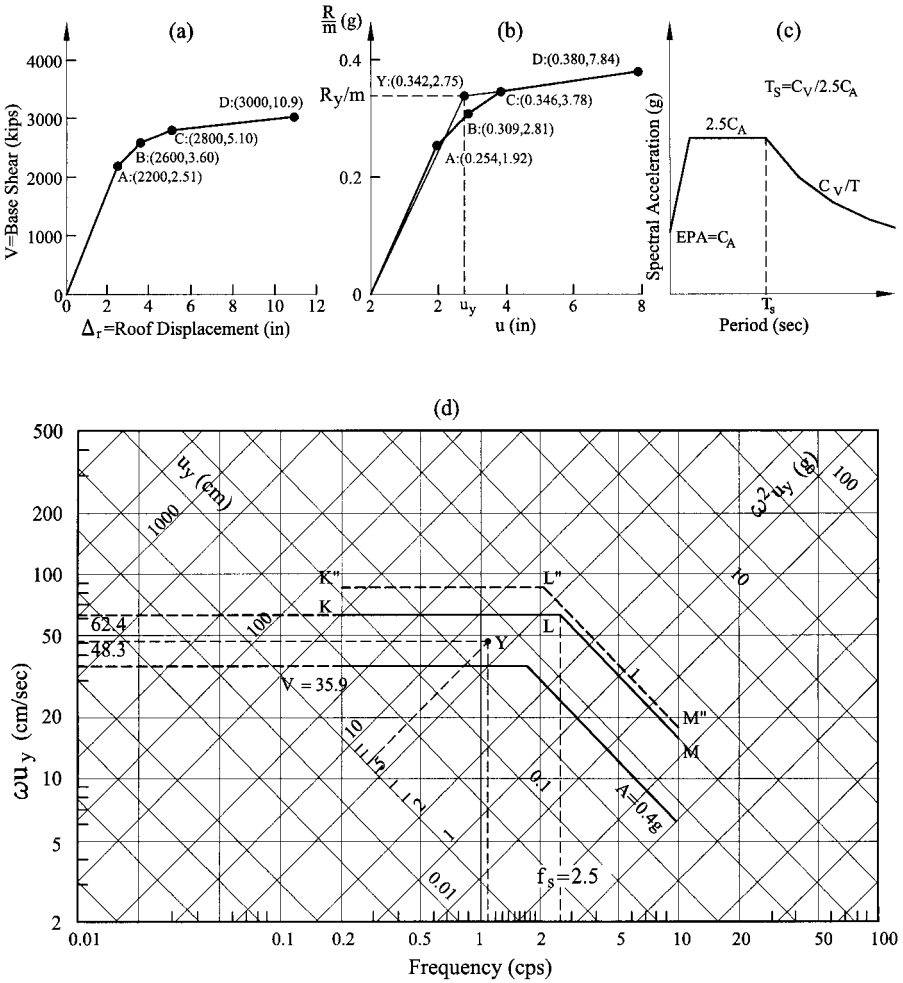

Figure 11. Example 1: (a) Push-over curve, (b) capacity diagram, (c) demand earthquake, (d) demand spectra.

is equivalent to A in this paper. C_V is the ordinate of the 5 per cent damped elastic design spectrum at $T = 1$ s. If the amplification factor $\psi_\mu = 1.74$ for $\mu = 1$ for the velocity region (Table VI) is assumed, the relation $\omega_s C_V = \omega_s \psi_\mu V = 2.5 C_A$ holds at $T = T_s$ (Figure 11(c)), with $T_s = C_V/2.5C_A$. For the first soil type $A = C_A = 0.4g$, $T_s = 0.4$ s and $\omega_s = 2\pi/T_s = 15.7$ rad/s, then $V = 1g/(15.7 \times 1.74) = 35.9$ cm/s. For the softer soil profile $A = C_A = 0.44g$, $T_s = 0.582$ s, $\omega_s = 10.8$ rad/s, and $V = 1.1g/(10.8 \times 1.74) = 57.4$ cm/s.

Example 1

(a) First, the same elastic spectrum considered in ATC-40 will be used. The corresponding ground motion, $A = 0.4g$ and $V = 35.9$ cm/s, is plotted in Figure 11(d). The spectral

regions of acceleration amplification (LM in Figure 10) and velocity amplification (KL in Figure 10) correspond in this case to $2.5A = 1g$ and $\psi_\mu V = 1.74 \times 35.9 = 62.4$ cm/s as shown in Figure 11(d).

(b) A bilinear model will be used. The model parameters must be selected to fit the capacity diagram (Figure 11(b)) up to the expected maximum response $u_{\max}$, so that the total area under the bilinear representation is equal to the area under the capacity diagram, i.e. equal energy is associated with both. In this case, a bilinear model with yield point Y with co-ordinates (0.342, 2.75) is chosen (Figure 11(b)). It must be pointed out that a precise fit to the capacity diagram is not compulsory. Indeed, a few tentative yield points and model shapes may be tried; since each system represents a single point in the tripartite spectrum, the sensitivity of the response to the model selection can be easily assessed.

(c) The chosen model has an elastic frequency $\omega = \sqrt{k/m} = \sqrt{R_y/u_y m} = \sqrt{0.342g/2.75} = 6.93$ rad/s, or $T = 2\pi/\omega = 0.907$ s (very close to the actual fundamental period of the building), or $f = 1.1$ cps. The model is represented in Figure 11(d) by point Y with tripartite co-ordinates: ($f = 1.1$, $u_y = 2.75'' = 6.98$ cm, $\omega u_y = 6.93 \times 6.98 = 48.3$ cm/s).

(d) The system is in the velocity region, and its ordinate features a reduction $\phi_\mu = 48.3/62.4 = 0.774$ with respect to the elastic spectrum. Using the relationship $\phi_\mu = (1.9\mu - 0.9)^{-0.7}$ a ductility response $\mu = 1.23$ is obtained (see Figure 9(b)).

(e) The maximum displacement of the equivalent system is $u_{\max} = \mu u_y = 1.23 \times 2.75 = 3.38'' = 8.6$ cm. This result is in very good agreement with the maximum displacement of 3.4″ calculated in the ATC-40 report. The observation can be made however that the inelastic spectrum procedure is considerably simpler than the ATC-40 method.

(f) The last step of the solution is to go back to estimate the displacement of the roof of the building. This is done using the above relation between u and Δ_r. According to the ATC-40 report calculations $F_1 \phi_{1,\text{roof}} = 1.31$, therefore $\Delta_r = 1.31 u_{\max} = 4.43'' = 11.3$ cm.

(g) In order to have an indication of the uncertainty underlying the estimated deformations and structural performance, it is recommended to consider a demand spectrum associated to a 0.159 probability of exceedance (response amplification associated to mean plus one standard deviation probability level). It is worth noting that for this verification the ground motion parameters that define the seismic hazard do not change, but the earthquake demand does change as a result of the other factors that influence the response, like the power, frequency content, and the duration of motion. Then, amplification factors $\psi_\mu + \sigma_\mu$ shall be used. In this case, factors of 2.84 and 2.39 are obtained from Table VI for the acceleration and velocity regions, respectively. The ordinates of the demand spectrum become $2.84A = 2.84 \times 0.4g = 1.136g$ and $2.39V = 2.39 \times 35.9 = 85.8$ cm/s, as shown by the dashed line K″L″M″ in Figure 11(d). (Note that the acceleration plateau of the initially given spectrum—Figure 11(c)—represented by line LM in Figure 11(d), actually corresponds to a response amplification level that exceeds the mean value, because it is quite close to the mean plus one standard deviation ordinate L″M″).

(h) The system is in the velocity region and features a reduction $\phi_\mu = 48.3/85.8 = 0.563$ from the elastic ordinate K″L″. Using the relationship $\phi_\mu = (1.9\mu - 0.9)^{-0.7}$ a ductility response $\mu = 1.67$ is obtained. The maximum displacement of the system, for a probability of exceedance of 0.16, is $u_{\max} = \mu u_y = 1.67 \times 2.75 = 4.6'' = 11.67$ cm. Note that this displacement is 36 per cent larger than that obtained in item (e) above.

(i) Similar to item (f) above, the roof displacement is $\Delta_r = 1.31 \times 11.67 = 15.3$ cm. Finally it is of interest to note that the example building is rather robust (3000 kips capacity for a total weight of 10540 kips); therefore, it experiences a mild inelastic response (low ductility) for the earthquake demands considered.

Example 2

(a) This example will be solved analytically without the aid of a figure. The ground motion in this case is $A = 0.44g$ and $V = 57.4$ cm/s, as calculated above. The elastic spectrum ordinates are $2.5A = 1.1g$ in the acceleration region and $\psi_\mu V = 1.74 \times 57.4 = 99.9$ cm/s in the velocity region.
(b) The system is represented by the same point determined above for Example 1 (point Y), with tripartite co-ordinates: ($f = 1.1$, $u_y = 2.75'' = 6.98$cm, $\omega u_y = 6.93 \times 6.98 = 48.3$ cm/s).
(c) The system is in the velocity region and presents a reduction $\phi_\mu = 48.3 \times 99.9 = 0.484$ with respect to the elastic spectrum. Then, the corresponding ductility is $\mu = 1.96$.
(d) The maximum displacement of the equivalent system is $u_{max} = \mu u_y = 1.96 \times 2.75 = 5.4''$ $= 13.7$ cm. In this case, the various ATC-40 procedures give maximum displacements from $5.5''$ to $6''$.
(e) The ordinates of the mean plus one standard deviation spectrum are in this case $2.84A = 1.25g$ in the acceleration region and $2.39V = 2.39 \times 57.4 = 137$ cm/s in the velocity region. The system is in the velocity region and presents a reduction factor $\phi_\mu = 48.3/137 = 0.3526$. The corresponding ductility response is $\mu = 2.81$, and the maximum displacement of the equivalent system is $u_{max} = \mu u_y = 2.81 \times 2.75 = 7.72'' = 19.6$ cm, i.e. 43 per cent larger than the displacement obtained for the spectrum shown in Figure 11(c).

CONCLUDING REMARKS

Performance-based seismic design requires explicit assessment of earthquake demands on structures, particularly inelastic deformations, to ensure they are within acceptable limits. Since methods for non-linear response history analysis of multi-degree-of-freedom buildings have not reached yet a stage of development to permit generalized use, simple approaches based on the response of single-degree-of-freedom (SDOF) systems have been proposed. The inelastic response of SDOF systems subjected to earthquakes can be directly and reliably estimated by means of the traditional Veletsos–Newmark–Hall procedure. This method may be considered to have at least the following advantages: (a) the earthquake demand is simply represented by the peak ground motion parameters—acceleration, velocity, and displacement—associated to probabilistically defined hazard levels, (b) responses correlate well with the peak ground motion parameters in each of the three characteristic spectral regions, providing better estimates than methods based on a single parameter, (c) the spectral ordinates are associated to known degrees of uncertainty, depending on the probability of exceedance of the factors selected to construct the demand spectrum, (d) no iterations or approximations are involved since spectral ordinates are based on actual inelastic responses, (e) inelastic design spectra can be derived for a variety of situations and conditions (tectonic environment, geotechnical setting, nearness

to source, etc.), the only limitation being the quality and quantity of the ground motion data available, and (f) the inelastic spectrum can be combined with the energy-dissipation spectrum [22] to account for damage related to the hysteretic behaviour, and estimates can be made of the ultimate deformation capacity of the structure required to meet a given performance level when subjected to a given design earthquake.

New factors for constructing demand spectra in the Veletsos–Newmark–Hall format were obtained for two large ensembles of earthquake records: Circumpacific Belt and California. With regard to the specific issues addressed in this study, the following conclusions were drawn: (a) the effect of the type of force–deformation relationship on the average response of non-linear systems is not significant, and responses can be conservatively predicted using the simple elastoplastic model, (b) the well known 'equal-displacement' and 'equal-energy' rules to relate elastic and inelastic responses are, on the average, unconservative for systems with moderate to large ductility. Improved rules that present better fit to the data considered are recommended. An example shows that inelastic deformations of SDOF systems can be directly obtained from a demand spectrum without considering the sequence of equivalent linear systems required by the ATC-40 procedures.

ACKNOWLEDGEMENTS

This study was carried out in the Department of Structural and Geotechnical Engineering at the Universidad Católica de Chile with financial assistance from the National Science and Technology Foundation of Chile (FONDECYT) under grant No. 1990112. The authors wish to thank Professor Wilfred Iwan of CALTECH for providing the reprocessed records of the Landers earthquake used in this study.

REFERENCES

1. Fajfar P, Krawinkler H (eds). *Nonlinear Seismic Analysis and Design of Reinforced Concrete Buildings*. Elsevier: Amsterdam, 1992.
2. Okada T. *Earthquake Resistance of Reinforced Concrete Structures—a Volume Honoring Hiroyuki Aoyama*. University of Tokyo Press: Tokyo, 1993.
3. Fillipou FC, Issa A. Nonlinear analysis of reinforced concrete frames under cyclic load reversals. *EERC* 88/12. University of California, Berkeley, 1988.
4. Applied Technology Council (ATC). *Seismic Evaluation and Retrofit of Concrete Buildings*. 1996; **1**:ATC-40.
5. Chopra AK, Goel R. Evaluation of NSP to estimate seismic deformations: SDF systems. *Journal of Structural Engineering*, ASCE 2000; **26-4**.
6. Veletsos AS, Newmark NM. Effect of inelastic behaviour on the response of simple systems to earthquake motions. *Proceedings of the 2nd World Conference on Earthquake Engineering*, vol. II, Japan, 1960; 895–912.
7. Veletsos AS, Newmark NM. Design procedures for shock isolation systems of underground protective structures, vol. III-response spectra of SDOF elastic and inelastic systems. *Report No. RTD* TDR-63-3096. Air Force Weapons Laboratory, Kirkland Air Force Base, New Mexico, June 1964.
8. Veletsos AS, Newmark NM, Chelapati CV. Deformation spectra for elastic and elastoplastic systems subjected to ground shock and earthquake motion. *Proceedings of the 3rd World Conference on Earthquake Engineering*, vol. II, New Zealand, 1965; 663–682.
9. Veletsos AS. Maximum deformation of certain non-linear systems. *Proceedings of the 4th World Conference on Earthquake Engineering*, vol. II, Chile, 1969; 156–170.
10. Newmark NM. Current trends in the seismic analysis and design of high-rise structures. In *Earthquake Engineering* (Chapter 16), Wiegel RL (ed.). Prentice-Hall Inc.: Englewood Cliffs, NJ, 1971; 403–424.
11. Newmark NM, Hall WJ. Procedures and criteria for earthquake resistant design, building practices for disaster mitigation. *National bureau of standards*, Building Science series, No. 46, vol. 1, Md., 1973; 209–236.

12. Riddell R, Newmark NM. Statistical analysis of the response of non-linear systems subjected to earthquakes. *Structural Research Series* No. 468. Department of Civil Engineering, University of Illinois, Urbana, Ill, 1979.
13. Newmark NM, Hall WJ. *Earthquake Spectra and Design*. Earthquake Engineering Research Institute, CA, 1982.
14. Riddell R, Newmark NM. Force–deformation models for non-linear analysis. *Journal of the Structural Division*, ASCE 1979; **105**:ST12.
15. Shakal A *et al.* CSMIP strong motion record from the Landers, California earthquake of 28 June 1992. *Report OSMS* 92-09. California Department of Conservation, Sacramento, 1992.
16. Iwan WD, Chen X. Important near-field ground motion data from the Landers earthquake. *Proceedings of the 10th European Conference on Earthquake Engineering*, vol. 1, Vienna, Austria, 1994.
17. Trifunac MD, Todorovska MI, Ivanovic SS. A note on distribution of uncorrected peak ground accelerations during the Northridge earthquake of January 1994. *Soil Dynamics and Earthquake Engineering*, vol. 13, Elsevier: Amsterdam, 1994.
18. Chopra AK. *Dynamics of Structures*. Prentice-Hall Inc.: Englewood Cliffs, NJ, 1995.
19. Riddell R. Inelastic design spectra accounting for soil conditions. *Earthquake Engineering and Structural Dynamics* 1995; **24**:1491–1510.
20. Mohraz B, Hall WJ, Newmark NM. A study of vertical and horizontal earthquake spectra. U.S. *Atomic Energy Commission Report WASH*-1255. Directorate of Licensing, April, 1973.
21. International Conference of Building Officials (ICBO). *Uniform Building Code*. Whittier, California, 1997.
22. Riddell R, García JE. Hysteretic energy spectrum and damage control. *Earthquake Engineering and Structural Dynamics* 2001; **30**:1791–1816.

